Electrochimica Acta 366 (2021) 137388

Contents lists available at ScienceDirect

Electrochimica Acta

journal homepage: www.elsevier.com/locate/electacta

Accurate measurement of internal resistance in microbial fuel cells by improved scanning electrochemical impedance spectroscopy

Bongkyu Kim[a,*], In Seop Chang[b], Richard M. Dinsdale[a], Alan J. Guwy[a]

[a] Sustainable Environment Research Centre (SERC), Faculty of Computing, Engineering and Science, University of South Wales, Pontypridd, Mid-Glamorgan CF37 1DL, UK

[b] School of Earth Sciences and Environmental Engineering, Gwangju Institute of Science and Technology (GIST), 123 Cheomdangwag-iro, Buk-gu, Gwangju 61005, Korea

ARTICLE INFO

Article history:
Received 24 July 2020
Revised 23 October 2020
Accepted 27 October 2020
Available online 30 October 2020

Keywords:
Microbial electrochemical system
Charge transfer resistance
Ohmic resistance
Mass transfer resistance
Over-potential
Voltage reversal

ABSTRACT

In this study, a scanning electrochemical impedance spectroscopy (EIS) technique is proposed to confirm the variation of internal resistance (R_{int}) including charge transfer resistance (R_{ct}) and ohmic resistance (R_{ohm}) under various working conditions of microbial fuel cells (MFCs). In order to establish a scanning EIS method, overall R_{int} of the system and R_{ct} of anode and cathode were measured by EIS under various external resistance conditions. Using this method, it was confirmed that the R_{ohm} and R_{ct} of each electrode changed variably. Based on the use of scanning EIS, the rapid increase in the R_{ct} of anode was found to be the main cause of a power-overshoot. As such, the use of scanning EIS is a methodology that can provide data to understand undesirable phenomena such as power-overshoot and voltage reversal which are generated by the typical operational characteristics of MFCs when used in scale up experiments. The use of scanning EIS should be applied as a novel measurement technique that improves on the use of the open circuit mode based EIS methods.

1. Introduction

Microbial fuel cells (MFCs) are an alternative energy harvesting system and wastewater treatment system which convert the chemical energy of the organic matter into electrical energy [1,2]. This technology has been attracting significant attention for the last two decades and efforts to advance the commercialization of this technology have intensified [3–6]. However, advances in electrochemical analysis methods to uncover the unique characteristics of MFC do not seem to keep pace with this goal of achieving commercialization. Unlike other electrochemical systems such as proton exchange membrane fuel cells and solid oxide fuel cells, the MFCs utilise electroactive microorganisms as live catalysts [1,3], so special considerations in understanding the characteristics of these biobased systems are required [7]. Especially, the maintenance and control of microbial kinetics of the biofilms found in the bio-electrodes of MFCs are challenging [8]. For instance, the power-overshoot and voltage reversal phenomena that are frequently generated in MFCs do not commonly occur in chemical fuel cells [9–11]. For example power-overshoot generated under anodic limitations such as electron depletion and proton accumulation [12–15]. Whilst the voltage reversal occurred due to operational kinetic imbalanced between serially connected MFCs [8,10]. These malfunctions usually only specifically occur mainly in MFCs. Therefore in order to understand these phenomena various electrochemical analysis methods such as the polarization test [10], linear sweep voltammetry [16], cyclic voltammetry [9] and electrochemical impedance spectroscopy (EIS) [13] have been introduced.

To date, the most frequently used electrochemical analysis technique to analyse the performance of MFCs is a discharge test including electrode potential measurement [17,18]. Electrochemical impedance spectroscopy (EIS) is also commonly conducted to measure the internal resistance (R_{int}) of MFCs [19]. The results measured in these ways have been interpreted to analyse the performance of MFCs and compare this with other MFCs. In the discharge test, improved developments have been made in the past two decades. Starting with the method of calculating the current and power by measuring only the voltage [20], and now to measuring the electrode potential together [17] by verifying the kinetic imbalance and limiting factor between each electrode [8, 18]. The potential difference of the separator, energy loss analysis and R_{int} analysis could also be conducted in the discharge test [21]. A man-

* Corresponding author. Present address at: Department of Chemical Engineering, University of Bath, Claverton Bath, Bath Avon BA2 7AY, United Kingdom.

E-mail addresses: b.kim0602@gmail.com, bk481@bath.ac.uk (B. Kim), ischang@gist.ac.uk (I.S. Chang), richard.dinsdale@southwales.ac.uk (R.M. Dinsdale), alan.guwy@southwales.ac.uk (A.J. Guwy).

https://doi.org/10.1016/j.electacta.2020.137388
0013-4686/

ual method for sequentially modifying the external resistance is widely used for the discharge test, but also a linear sweep voltammetry method using a potentiostat can be used [19]. In addition, effect of the direction of charge and discharge in the analytical procedure on the performance results of MFCs has also been investigated [22].

In terms of measurement of R_{int} of MFCs, a resistance calculation method using the slope of the V-I curve (electrode potential slope analysis, EPS) collected through a discharge test [18,23,24] and EIS analysis are mainly used [25–28]. The R_{int} is calculated from the slope of the V-I curve and can provide a reliable R_{int} value from MFCs having ohmic resistance (R_{ohm}), which includes the solution/contact resistance, and other main resistances of the cell [18,29,30]. It would be difficult to distinguish each particular resistance such as the charge transfer resistance (R_{ct}) for each electrode, the mass transfer resistance, the solution resistance, and the membrane resistance from the value of calculated R_{int} by EPS. Also, in the case of R_{int} values obtained from the peak power point calculation method [31], each R_{ct}, R_{ohm}, and R_m value could not be distinguished. Thus, EIS was introduced as an alternative method to complement this method [32]. EIS measurements are a way to identify the R_{int} of the diverse MFC's structure. The R_{ct} of each electrode (*via* the three-electrode measurement method), the R_{ohm} including solution/contact resistance (*via* the two-electrode measurement method), and the membrane resistance (*via* the four-electrode measurement method) was determined. EIS determinations are most commonly measured in the open circuit mode (OCM) for the cell [33]. However, since it is measured in a system operated by OCM, only the values for R_{ct} and R_{ohm} (including solution/contact resistance) for open circuit voltage (OCV) can be obtained. In fact, the power-overshoot and voltage reversal generally occur in the relatively low external resistance area and relatively high current production region [12, 34]. Especially, power-overshoot is a phenomenon that occurs in the process of discharge test [12]. As the external resistance decreases, the underlying capacity of current production returns but the expected increase in current does not. Therefore, to understand the power-overshoot, EIS measurements based on OCV is unsuitable. In addition, since voltage reversal is caused by the imbalance of the conditions for current production [8], to attempt the analysis based on EIS measurement based on OCV is not appropriate.

Furthermore, since a close circuit voltage (CCV) measured while the MFC is producing current is claimed to be the working voltage of the MFC, it is doubtful whether the R_{int} measured under OCM is suitable for measuring the actual R_{int} of a working MFC. In MFCs, this issue was highlighted by Motos et. al., who presented an analysis of a range of over-potentials under various external resistance conditions in MFCs [21]. According to these authors, the R_{int} as well as over-potentials of the anode and cathode are affected by changes in external resistance with the key elements affecting the potential loss in each situation also changing.

Therefore, in this study, a novel scanning EIS approach is proposed and developed to understand the inherent performance phenomenon for MFCs. Based on the principle of potentiostatic EIS, it was conducted under various working conditions. It is expected to be able to confirm the variable internal resistance would be based on the EIS measured under various external resistances which form various working voltages. Therefore, it is called scanning EIS to describe EIS measured by various working voltages which change in stages. The change in the R_{int} including R_{ct} which is occurring under various external resistance conditions, within the range of various voltages and currents, is measured with the scanning EIS approach. As a result, this would clarify the underlying mechanism of the phenomenon of power-overshoot through the scanning EIS analysis conducted under a discharge test regime. It enhances the benefit of the proposed novel scanning EIS measurement technology. Finally, it is proposed that R_{int} including R_{ohm} and R_{ct} be an additional criterion together with discharge test for evaluating the performance of the MFCs systems.

2. Experimental

2.1. MFC construction

The MFCs were configured as a two-chamber unit using cube type acrylic reactors. The working volume of the two chamber MFC is 80 ml, and each chamber is approximately 40 ml (external dimensions: 6 cm of wide x 5 cm of length x 5 cm of height, and interior is cylindrical with a diameter of 3 cm). A plain carbon cloth (CCP40, Fuel Cell Earth, MA, USA) was used as the anode electrode and 40%Pt/c-coated carbon cloth (0.5mg/cm^2) (EC40-19, Fuel Cell Earth, MA, USA) as the cathode electrode. To develop and demonstrate the proposed scanning EIS methodology, MFC 1 using a cation exchange membrane (CEM, CMI-7000S, Membrane International Inc., NJ, USA) was constructed and studied, then the membrane was exchanged to an anion exchange membrane (AEM, AMI-7001S, Membrane International Inc., NJ, USA) to confirm the feasibility of the scanning EIS in other MFC materials that are widely used in MFC research. To reduce the internal resistance between the anode and the cathode, the two electrodes were fitted closely to both sides of membrane with no or litter gap. In order to measure the potential of each electrode, a 4-electrode system was constructed with two identical reference electrodes (RE) (MF-2052, BASi Co., IN, USA) and were installed at less than 5 mm distance between the reference and working electrode (anode and cathode).

2.2. Inoculation and operation

In order to develop the bio-anode of the MFCs, an effluent from the anode compartment of the existing MFC system was used as the inoculum source. The MFCs were operated in circulation batch mode for the inoculation process. After the bio-anode was fully developed, it was operated in the continuous mode under a hydraulic retention time of 2.5 h. To prevent a performance limitation due to substrate depletion at the bio-anode, synthetic wastewater containing a high concentration of acetate (40 mM) was used as anolyte (pH 7.2, conductivity of 9 mS/cm) which prepared with same recipe [35]. The cathode compartment contained 50 mM phosphate buffer solution (pH 7.2, conductivity of 6.6 mS/cm). Under continuous mode operation, the discharge test of the MFCIwas performed first, and then multiple external resistors were selected to measure the scanning EIS values based on the discharge test results. The OCV was charged for 0.5 h for the discharge test and then the following external resistance chosen for a sequence of 12 resistors (100 kΩ, 50 kΩ, 30 kΩ, 10 kΩ, 5 kΩ, 3 kΩ, 1 kΩ, 0.5 kΩ, 0.3 kΩ, 0.1 kΩ, 0.05 kΩ, 0.03 kΩ). The interval between each resistor change was 5 minutes. This procedure was performed twice to collect duplicate data. Based on the discharge test results, the test resistances for scanning EIS method were selected as 100 kΩ, 10 kΩ, 1 kΩ, 0.3 kΩ, 0.1 kΩ, and 0.03 kΩ respectively. To conduct the scanning EIS, the EIS was measured under external resistance condition (CCV). Under 100 kΩ of external load, the voltage and electrode potential were monitored until a stabilized value for at least 15 min was shown, and then the EIS measurement was performed. After the EIS measurement, to confirm that the voltage and electrode potentials were still stable they monitored again for 15 min. Then the external resistance was changed to 10 kΩ which was then the next selected external load, and then the same procedure was repeated. After each test on each external load was completed, the load was changed to the next sequential resistor, and the same process was repeated until 0.03 kΩ was reached. After completed the experiment with MFCI, the membrane was replaced

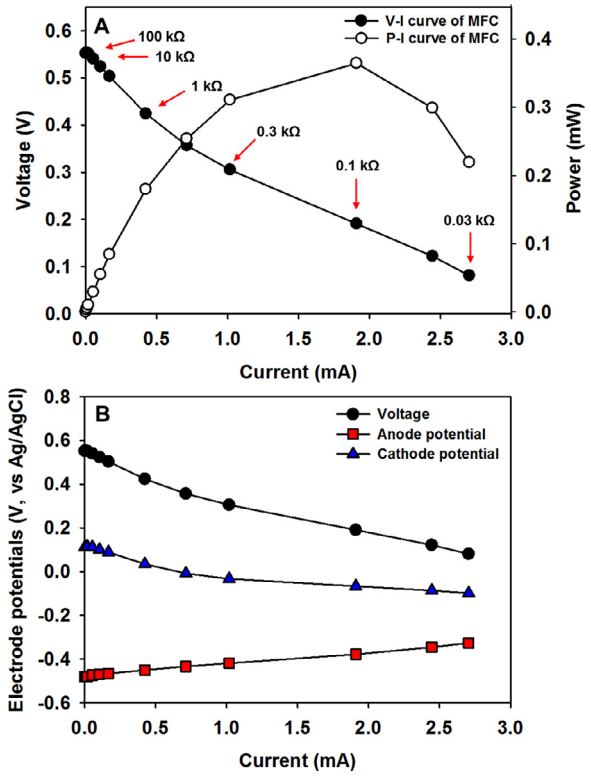

Fig. 1. (A) V-I and P-I curves and (B) electrode potentials curves for MFCI, which using CEM, of the discharging tests measured with 12 resistances. The indicated six external resistances were selected to develop scanning EIS.

with a AEM material. The MFCII was then stabilised for one week and then the experiment was repeated under the same methodology as used for the MFCI. The voltage (V) measured at the external resistor (R) in the discharge test was converted into current (I) and power (P) based on Ohm's law (V=IR) and Joule's first law. Based on this, the V-I curve and the P-I curve were derived.

2.3. EIS measurement and analysis

The EIS measurements used to determine the R_{int} were collected through a potentiostat equipped with a frequency analysis module (FDA) (VersaSTAT 3, Princeton Applied Research, USA). In order measure the overall R_{int} of the MFC, it measured in the two-electrode measurement method with anode and cathode. To measure the R_{ct} of each electrode, it was measured by the three-electrode measurement method with reference electrode. The EIS was measured under a frequency of 10kHz to 0.1 Hz and with an amplitude of 10 mV. To verify the measured results, each measurement was performed in duplicate, and the points where an overload occurred on the derived results were removed for the data analysis. To present the EIS results of MFCII system, the measured circuit is reformed by inverting the data (Fig. S1). For the calculation of the R_{ohm} and the R_{ct} of the anode and cathode, the R_{ct} value was determined by the "semi-circular" Nyquist plot measurement in the Vesrastudio program (Princeton Applied Research, USA) and the R_{ohm} was calculated from the value of solution resistance of EIS data of the entire cells.

3. Results and discussion

3.1. Performance evaluation and R_{int} calculation by discharge test

Fig. 1 presents the discharge test measurement based on 12 applied external resistances after the MFCI had stabilized. The MFCIhas maximum power of 0.371±0.006 mW and maximum current of 2.727±0.022 mA. Based on the slope calculation method of V-I curve [23,24], Overall R_{int} was calculated as around 135 Ω, and each anode and cathode resistance was calculated to be around 53 Ω and 43 Ω (membrane resistance, which was measured potential difference between two reference electrode, was calculated to be around 38 Ω, data is not present). Also, from the P-I curve with peak power point calculation method [31], the R_{int} was calculated as approximately 100 Ω. But these calculated R_{int} cannot be distinguished as R_{ct} and R_{ohm} separately because it represents total R_{int} at the point of system. To understand more clearly the situation of R_{int} of MFCs under working condition, measure for R_{int} should be conducted under each external resistance condition. Therefore, the scanning EIS method was established. In order to have the same quality of data that could be collected more efficiently in a shorter time, several representative external resistances were selected from discharge test two each from the high, middle, and low current production regions. Measuring EIS across all 12 resistors is time consuming, which can also be stressful to the electroactive microorganisms in the bioanode. Also, from a bioreactor's point of view, to suitable measuring time is required in order to minimize the variables that could change the anode performance during long-term measurements.

3.2. R_{int} measured by scanning EIS

In order to facilitate the scanning EIS method, the R_{int} of the whole cell and the R_{ct} of each electrode were measured under each selected external resistance (Fig. 2). During the scanning EIS, the measured voltage and electrode potentials was described in Fig. S2. The entire R_{int}, including R_{ct} and R_{ohm}, is affected according to the external resistance and was verified. R_{ohm} (the represented solution resistance) tended to decrease with decreasing external resistance (Fig. 2A). As the external resistance decreases, the current production of the MFC was increased, i.e., the movement of electrons and corresponding ions between anode and cathode was increased. The movement of ions in solution might affect the decreased the R_{int}. Since all electrodes including reference electrode were fixed in the reactor and their own material resistance of system was not changed, the electrolyte is the remaining factor that might affect the decreased R_{int}. The local conductivity increase in the system might be expected to occur due to this migration effect by the stream of the electrolyte to match the charge balance and the movement of electrons by the potential difference. In terms of R_{ct}, it was confirmed that the R_{ct} value decreased in the whole cell (two electrodes EIS), and the same result was also obtained in the R_{ct} measurement of the electrodes performed in three electrodes EIS, to verify this (Fig. 2B and C). When reducing the external resistance, R_{ct} was also reduced, as it is closely related in conjunction with the increase in current. As more electrons move between the anode and the cathode, more redox reactions occur and the R_{ct} decreases. Therefore, in the case of the MFCI that produced a stable current, the R_{ct} of the anode and cathode tended to decrease gradually as the external resistance decreased (as the current also increased) as well as R_{ohm} generated between the working electrode and reference electrode also similarly followed a similar trend. Therefore, as such, the R_{int} is affected and determined by the MFC's working conditions.

3.3. R_{int} analysis and R-I curve

In Table 1, the summary the value of R_{int} of each item, calculated based on the Nyquist plots measured through the EIS is shown. Under the various external resistance condition, as the current increases and the voltage decreases, all R_{ohm} and R_{ct} values tend to decrease. When comparing the values at 100 kΩ and

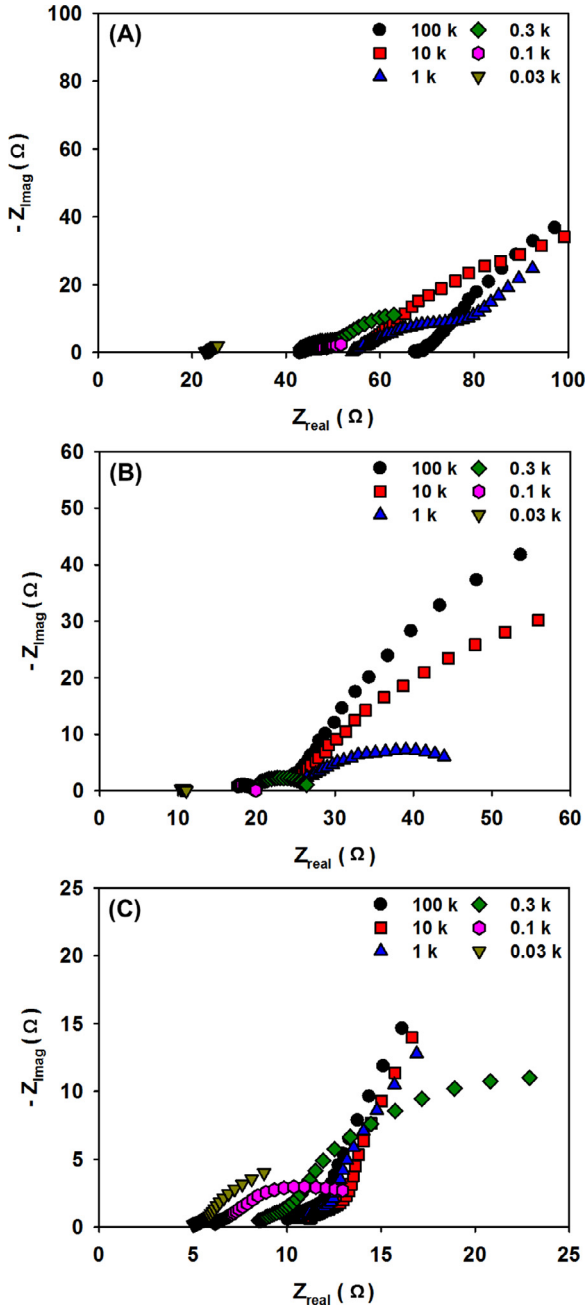

Fig. 2. Nyquist plots obtained from the scanning EIS tests conducted the selected six external resistances in MFCI. (A) the overall R_{int} was measured by two electrode EIS method and R_{ct} of (B) anode and (C) cathode was measured by three electrode EIS method.

Table 1
Calculated each R_{int} (R_S and R_{CT} of anode/cathode) to overall (sum of each) R_{int} at different external resistors in MFCI.

R_{ext}	R_{ohm}	$R_{ct\ of\ Anode}$	$R_{ct\ of\ Cathode}$	Overall R_{int}*
100 k	67	145	327	539
10 k	55	137	296	488
1 K	53	30	104	187
0.3 K	41	9.4	29	79.4
0.1 K	42	4.2	10	56.2
0.03 K	22	1.0	13	36.0

* Overall R_{int}: sum of R_{ohm}, $R_{ct\ of\ Anode}$, and $R_{ct\ of\ Cathode}$

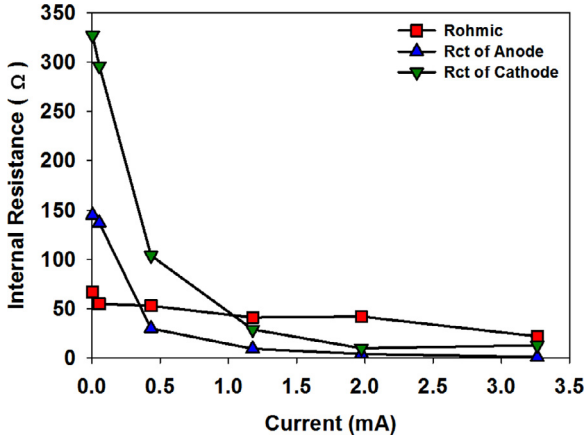

Fig. 3. R_{Int}-I curves produced from the proposed scanning EIS under six selected resistors in MFCI. In the same context as the I-V, P-I, and EP-I curve, R_{int}-I shown to be able to analyze the performance of system.

0.03kΩ, all R_{int} have undergone a tremendous change, R_{ohm} is from 67 Ω to 22 Ω, the R_{ct} of anode is from 145 Ω to 1 Ω, the R_{ct} of cathode is from 327 Ω to 13 Ω. In Fig. 3. Data was plotted to compare the tendency and proportion of each R_{int} items under current production verses the current (R-I curve). Initially the R_{ct} of cathode is the largest, but as the current becomes more than 1 mA, the R_{ohm} has the highest weight as the R_{ct} decreases. This tendency is in line with the theory that in the V-I curve the low current region is defined as the R_{ct} region, and then the region producing stable current is defined as the R_{ohm} region. Based on the slope calculation method from the I-V curve in Fig. S2, overall R_{int} was calculated as around 77 Ω near the high current region. This, value is not significantly different from the overall value for R_{int} (Table 1) under the external loads selected from the high current area (0.1 kΩ and 0.03kΩ). Unlike the calculated total R_{int} from the V-I curve, the value of each item would be distinguished in this proposed scanning EIS method. Thus, based on the proposed analysis, the part to be improved in the operational condition of MFCs could be confirmed. In order to further improve the efficiency in the operation of the MFCs in this study, reducing the Rohm such as from the electrode resistance is an effective way to enhance the electrode performance.

3.4. Determination of power-overshoot by scanning EIS

The proposed scanning EIS technique can be used to understand the deleterious events such as power-overshoot in MFCs. Fig. 4 shows that the power-overshoot event occurred during discharge test based on selected resistors in MFC II. The power-overshoot was generated at a low external resistance from 0.1 kΩ, i.e. in the high current region. The cause of the power-overshoot is potentially caused by the anode limitation such as electron depletion phenomenon due to proton accumulation and limitation of substrates, poor enrichment of the biofilm [12,13,15,36,37]. There are many mechanisms proposed for the cause of power-overshoot, but full understanding of the phenomenon during discharge tests is not yet fully understood. In this context, the scanning EIS method would expect to expand on the limited information of this phenomena when the power-overshoot occurs during discharge test. The scanning EIS results are presented in Fig. 5. and Table S1. As with the results of the discharge test, interesting results were obtained at 0.1 kΩ. As shown in Fig. 5B, as the external resistance step by step decreases, the R_{ct} of the anode gradually decreases from 136 Ω (at 100 kΩ) to 23 Ω (at 0.3 kΩ), but then sharply increased to 106 Ω at 0.1 kΩ of external resistance (the point where

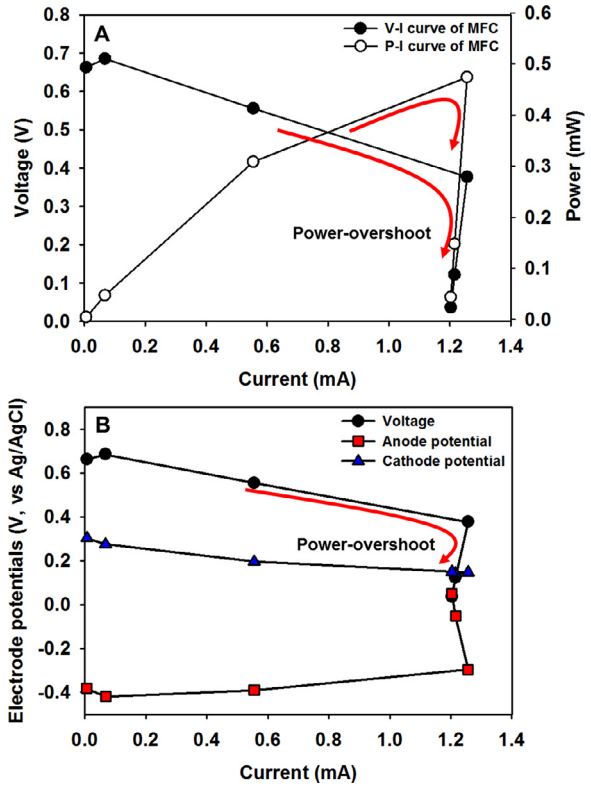

Fig. 4. (A) V-I and P-I curves and (B) electrode potentials curves for MFCII, which using AEM, of the discharging tests measured with six selected resistances. A power-overshoot is generated in high current region.

power-overshoot occurs). Unlike the R_{ct} of the anode, the R_{ct} of cathode was maintained and decreased from 514 Ω to 1 Ω. The R_{ohm} decreased from 87 Ω to 23 Ω (Fig. 5A). As a result, the tendency of R_{ct} of the anode is closely related to the power-overshoot that occurred during the discharge test. The R_{ct} of the anode appears to be making a reversal while tracking towards the minimum. The increase of R_{ct} could be described as a malfunction of bio-anode's electroactive microorganisms. An failure of the electron transfer process of electroactive microorganisms which mainly effects the R_{ct} of the anode is due to a set of complex process interactions [38]. Also, the R_{ct} could be affected by mass-transfer phenomenon and proton accumulation [13, 15, 27]. Power overshoot caused by the lack of substrate might represent an increase in R_{ct} by reduced mass-transfer. Also, proton accumulation would show similar symptoms to power-overshoot caused by electron depletion. However, the exact cause could not be identified in this study. Based on this study, the R_{ct} was found to increases instantly during the discharge test and could be just added as one of the causes of the power-overshoot. Whether the R_{ct} increased rapidly due to other factors or that the R_{ct} of the bio-anode increased sharply and influenced the performance, is unclear and it should be additionally investigated in MFCs.

3.5. Establishment of scanning EIS technique for MFCs

In this study, the scanning EIS technique was shown to confirm the verification of R_{int} in MFCs. In practice, the currently used EIS technique is measured using the OCM mode [32, 33], theoretically with no current (electrons) being produced or only with very small amounts of current (electrons) for practical measurement in the measuring equipment. Besides, generally OCV is not considered as a good indicator of the performance of the MFC system. Rather, the MFC has a high OCV (typically greater than 0.6 V, sometimes

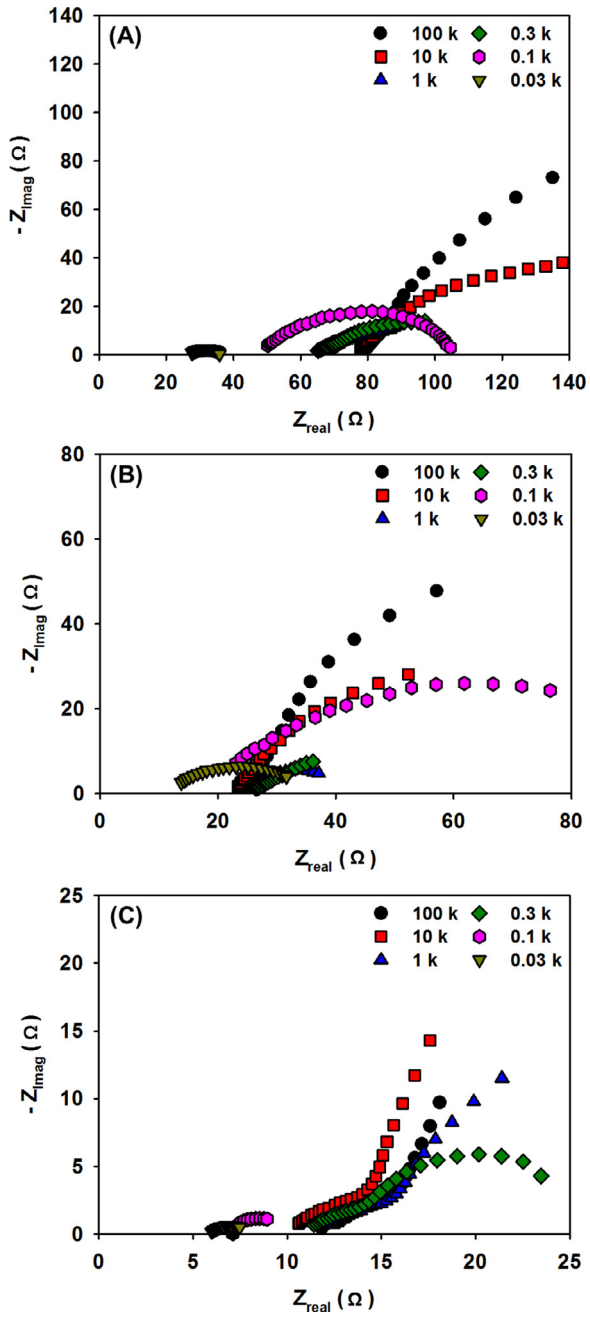

Fig. 5. Nyquist plots obtained from the scanning EIS tests conducted the selected six external resistances in MFCII. (A) the overall R_{int} was measured by two electrode EIS method and R_{ct} of (B) anode and (C) cathode was measured by three electrode EIS method.

even 1 V), but the actual operating voltage is much lower (0.2 to 0.5 V). Thus, it is argued that the R_{int} should be measured according to close-circuit voltage (not the OCV condition) based on each external resistance (potential condition) used. As with the results measured in this study, the results of the R_{int} determined under the condition of each external resistance (in other words, under different potential conditions) are different. Therefore, it is suggested from the results here to use R_{int} values measured via scanning EIS for correct comparison and evaluation of MFCs. In addition, in future to achieve better characterisation and analysis of MFCs, the conventional R_{int} calculation method using the V-I curve and peak power calculation method would need be replaced by the methodology proposed here, where the specific R_{ct} and R_{ohm} are

calculated. The R_{ct}, R_{ohm}, and R_m regions are distinguished through the use of the V-I curve and calculated from Ohm's law, but it is concluded that it is not possible to directly calculate the intrinsically changing R_{int} under changing external resistors. Therefore, it is necessary to measure the R_{int} of each external resistor based on the scanning EIS and the R-I curve could then be used to understand the change of R_{int} under current production. In the same context as presenting the discharge test results with the V-I curve and the E-I curve, the EIS results which represent the R_{int} of the entire system and the separated R_{ct} of the anode and the cathode should be presented together as shown in Fig. 3. It is possible to more clearly distinguish where the performance enhancement in each system has been effective or not.

In this study, it is very interesting that the value of the R_{int} of each part and the entire cell that make up the system at each external resistor changes. Thus, it is once again worth considering whether the R_{int} presented by measuring the EIS based on OCV means the true R_{int} of the system is determined and should be an objective of future work. In addition, the area of scanning EIS could analyse and interpret special phenomena, frequently occurring only in MFCs, for example, voltage reversal, short circuit, and the power-overshoot.

4. Conclusion

This study successfully explored and identified the effectiveness of the proposed R_{int} methodology. The scanning EIS technique was able to determine the overall R_{int} of system as well as R_{ct} of each electrode under various applied external resistances. Based on the finding that all R_{int} values are biased when the application of each external resistor is changed, therefore the need to refresh the base point of R_{int} has been confirmed. For further exploitation and commercialization of MFCs, an accurate understanding of R_{int} must be evaluated, and the proposed scanning EIS in this study was found to be suitable for this process.

Declaration of Competing Interest

The authors declare that they have no known competing financial interests or personal relationships that could have appeared to influence the work reported in this paper.

Credit authorship contribution statement

Bongkyu Kim: Conceptualization, Methodology, Validation, Formal analysis, Investigation, Writing - original draft, Writing - review & editing, Supervision. **In Seop Chang:** Conceptualization, Funding acquisition, Writing - original draft, Writing - review & editing. **Richard M. Dinsdale:** Project administration, Funding acquisition, Writing - original draft, Writing - review & editing. **Alan J. Guwy:** Project administration, Funding acquisition, Writing - original draft, Writing - review & editing.

Acknowledgments

This work was supported by the EPSRC Multi-disciplinary fuels, RCUK Energy programme, Liquid fuels and bioenergy from CO2 Reduction (Lifes-CO2R) project [EP/N009746/1], the FLEXIS research project [grant number: WEFO 80835], and National Research Foundation of Korea (NRF), funded by the Korean Government (2020R1A2C3009210). Dinsdale would also like to acknowledge the Royal Academy of Engineering Fellowship Chair in Emerging Technologies - CiET1819/2/86.

Supplementary materials

Supplementary material associated with this article can be found, in the online version, at doi:10.1016/j.electacta.2020.137388.

References

[1] B. Kim, J. An, D. Fapyane, I.S. Chang, Bioelectronic platforms for optimal bio-anode of bio-electrochemical systems: from nano-to macro scopes, Bioresour. Technol. 195 (2015) 2–13.
[2] M. Sun, L.-F. Zhai, W.-W. Li, H.-Q. Yu, Harvest and utilization of chemical energy in wastes by microbial fuel cells, Chem. Soc. Rev. 45 (2016) 2847–2870.
[3] Z. He, Microbial Fuel Cells: Now Let us Talk About Energy, ACS Publications, 2012.
[4] W.-W. Li, H.-Q. Yu, Utilization of Microbe-Derived Electricity for Practical Application, ACS Publications, 2013.
[5] H. Wang, J.-D. Park, Z.J. Ren, Practical energy harvesting for microbial fuel cells: a review, Environ. Sci. Technol. 49 (2015) 3267–3277.
[6] J.R. Trapero, L. Horcajada, J.J. Linares, J. Lobato, Is microbial fuel cell technology ready? An economic answer towards industrial commercialization, Appl. Energy 185 (2017) 698–707.
[7] S. Choi, B. Kim, I.S. Chang, Tracking of Shewanella oneidensis MR-1 biofilm formation of a microbial electrochemical system via differential pulse voltammetry, Bioresour. Technol. 254 (2018) 357–361.
[8] B. Kim, S.V. Mohan, D. Fapyane, I.S. Chang, Controlling Voltage Reversal in Microbial Fuel Cells, Trends in Biotechnology, 2020.
[9] X. Zhu, J.C. Tokash, Y. Hong, B.E. Logan, Controlling the occurrence of power overshoot by adapting microbial fuel cells to high anode potentials, Bioelectrochemistry 90 (2013) 30–35.
[10] J. An, H.S. Lee, Occurrence and implications of voltage reversal in stacked microbial fuel cells, ChemSusChem 7 (2014) 1689–1695.
[11] B. Kim, B.G. Lee, B.H. Kim, I.S. Chang, Assistance current effect for prevention of voltage reversal in stacked microbial fuel cell systems, ChemElectroChem 2 (2015) 755–760.
[12] B. Kim, J. An, I.S. Chang, Elimination of power overshoot at bioanode through assistance current in microbial fuel cells, ChemSusChem 10 (2017) 612–617.
[13] S. Jung, M.M. Mench, J.M. Regan, Impedance characteristics and polarization behavior of a microbial fuel cell in response to short-term changes in medium pH, Environ. Sci. Technol. 45 (2011) 9069–9074.
[14] A.E. Franks, K.P. Nevin, H. Jia, M. Izallalen, T.L. Woodard, D.R. Lovley, Novel strategy for three-dimensional real-time imaging of microbial fuel cell communities: monitoring the inhibitory effects of proton accumulation within the anode biofilm, Energy Environ. Sci. 2 (2009) 113–119.
[15] C.I. Torres, A. Kato Marcus, B.E. Rittmann, Proton transport inside the biofilm limits electrical current generation by anode-respiring bacteria, Biotechnol. Bioeng. 100 (2008) 872–881.
[16] V.J. Watson, B.E. Logan, Analysis of polarization methods for elimination of power overshoot in microbial fuel cells, Electrochem. Commun. 13 (2011) 54–56.
[17] B.E. Logan, E. Zikmund, W. Yang, R. Rossi, K.-Y. Kim, P.E. Saikaly, F. Zhang, Impact of ohmic resistance on measured electrode potentials and maximum power production in microbial fuel cells, Environ. Sci. Technol. 52 (2018) 8977–8985.
[18] R. Rossi, B.P. Cario, C. Santoro, W. Yang, P.E. Saikaly, B.E. Logan, Evaluation of electrode and solution area-based resistances enables quantitative comparisons of factors impacting microbial fuel cell performance, Environ. Sci. Technol. 53 (2019) 3977–3986.
[19] F. Zhao, R.C. Slade, J.R. Varcoe, Techniques for the study and development of microbial fuel cells: an electrochemical perspective, Chem. Soc. Rev. 38 (2009) 1926–1939.
[20] J.K. Jang, T.H. Pham, I.S. Chang, K.H. Kang, H. Moon, K.S. Cho, B.H. Kim, Construction and operation of a novel mediator-and membrane-less microbial fuel cell, Process Biochem. 39 (2004) 1007–1012.
[21] P. Rodenas Motos, A. ter Heijne, R. van der Weijden, M. Saakes, C.J. Buisman, T.H. Sleutels, High rate copper and energy recovery in microbial fuel cells, Front. Microbiol. 6 (2015) 527.
[22] N. Degrenne, P. Ledezma, P. Bevilacqua, F. Buret, B. Allard, J. Greenman, I. Ieropoulos, Bi-directional electrical characterisation of microbial fuel cell, Bioresour. Technol. 128 (2013) 769–773.
[23] B.E. Logan, B. Hamelers, R. Rozendal, U. Schröder, J. Keller, S. Freguia, P. Aelterman, W. Verstraete, K. Rabaey, Microbial fuel cells: methodology and technology, Environ. Sci. Technol. 40 (2006) 5181–5192.
[24] R. Rossi, B.E. Logan, Unraveling the contributions of internal resistance components in two-chamber microbial fuel cells using the electrode potential slope analysis, Electrochim. Acta (2020) 136291.
[25] Z. He, N. Wagner, S.D. Minteer, L.T. Angenent, An upflow microbial fuel cell with an interior cathode: assessment of the internal resistance by impedance spectroscopy, Environ. Sci. Technol. 40 (2006) 5212–5217.
[26] X. Dominguez-Benetton, S. Sevda, K. Vanbroekhoven, D. Pant, The accurate use of impedance analysis for the study of microbial electrochemical systems, Chem. Soc. Rev. 41 (2012) 7228–7246.
[27] R. Rossi, D.M. Hall, X. Wang, J.M. Regan, B.E. Logan, Quantifying the factors limiting performance and rates in microbial fuel cells using the electrode potential slope analysis combined with electrical impedance spectroscopy, Electrochim. Acta (2020) 136330.

[28] A. Ter Heijne, D. Liu, M. Sulonen, T. Sleutels, F. Fabregat-Santiago, Quantification of bio-anode capacitance in bioelectrochemical systems using electrochemical impedance spectroscopy, J. Power Sources 400 (2018) 533–538.
[29] Y. Fan, E. Sharbrough, H. Liu, Quantification of the internal resistance distribution of microbial fuel cells, Environ. Sci. Technol. 42 (2008) 8101–8107.
[30] P. Liang, X. Huang, M.-Z. Fan, X.-X. Cao, C. Wang, Composition and distribution of internal resistance in three types of microbial fuel cells, Appl. Microbiol. Biotechnol. 77 (2007) 551–558.
[31] S. Cheng, H. Liu, B.E. Logan, Increased power generation in a continuous flow MFC with advective flow through the porous anode and reduced electrode spacing, Environ. Sci. Technol. 40 (2006) 2426–2432.
[32] Z. He, F. Mansfeld, Exploring the use of electrochemical impedance spectroscopy (EIS) in microbial fuel cell studies, Energy Environ. Sci. 2 (2009) 215–219.
[33] A.K. Manohar, O. Bretschger, K.H. Nealson, F. Mansfeld, The use of electrochemical impedance spectroscopy (EIS) in the evaluation of the electrochemical properties of a microbial fuel cell, Bioelectrochemistry 72 (2008) 149–154.
[34] B. Kim, I.S. Chang, Elimination of voltage reversal in multiple membrane electrode assembly installed microbial fuel cells (mMEA-MFCs) stacking system by resistor control, Bioresour. Technol. 262 (2018) 338–341.
[35] J.R. Kim, G.C. Premier, F.R. Hawkes, R.M. Dinsdale, A.J. Guwy, Development of a tubular microbial fuel cell (MFC) employing a membrane electrode assembly cathode, J. Power Sources 187 (2009) 393–399.
[36] Y. Hong, D.F. Call, C.M. Werner, B.E. Logan, Adaptation to high current using low external resistances eliminates power overshoot in microbial fuel cells, Biosens. Bioelectron. 28 (2011) 71–76.
[37] P.-C. Nien, C.-Y. Lee, K.-C. Ho, S.S. Adav, L. Liu, A. Wang, N. Ren, D.-J. Lee, Power overshoot in two-chambered microbial fuel cell (MFC), Bioresour. Technol. 102 (2011) 4742–4746.
[38] B.E. Logan, R. Rossi, P.E. Saikaly, Electroactive microorganisms in bioelectrochemical systems, Nat. Rev. Microbiol. 17 (2019) 307–319.